Conjectured orbital ordering behavior of $Nd_{0.5}Sr_{0.5}MnO_3$ under high pressures

R. C. Yu[a)]
Chinese Academy of Sciences, Key Laboratory of Extreme Conditions of Physics, Institute of Physics, P.O. Box 603, Beijing 100080, China
and Department Earth and Planetary Science, University of California, Berkeley, CA 94720-4767

J. Tang
National Institute for Materials Science, 1-2-1 Sengen, Tsukuba 305-0047, Japan

L. D. Yao
Chinese Academy of Sciences, Key Laboratory of Extreme Conditions of Physics, Institute of Physics, P.O. Box 603, Beijing 100080, China

A. Matsushita
National Institute for Materials Science, 1-2-1 Sengen, Tsukuba 305-0047, Japan

Y. Yu, F. Y. Li, and C. Q. Jin
Chinese Academy of Sciences, Key Laboratory of Extreme Conditions of Physics, Institute of Physics, P.O. Box 603, Beijing 100080, China

(Received 11 August 2004; accepted 10 January 2005; published online 11 April 2005)

We have synthesized $Nd_{0.5}Sr_{0.5}MnO_3$ polycrystalline bulk samples by solid state reaction, which show ferromagnetic (FM), *A*-type antiferromagnetic (AF) and charge ordering charge exchange (CE)-type AF transitions on cooling from room temperature to 78 K. We consider that the abundant magnetic structures are caused by phase segregation. We have investigated and conjectured the orbital ordering behavior under hydrostatic pressures up to 7.5 GPa and found that low pressure favors the *A*-type AF phase with $d(x^2-y^2)$ orbital ordering and the CE-type AF phase with $d(3x^2-r^2)/d(3y^2-r^2)$ orbital ordering, while suppressing the FM phase with disordered orbital ordering; however, high pressure favors the *A*-type phase and suppresses the CE-type AF phase. Transport property enhancement and large resistance changes under high pressures are observed. © *2005 American Institute of Physics*. [DOI: 10.1063/1.1866481]

I. INTRODUCTION

The colossal magnetoresistance (CMR) effect, simultaneously including a ferromagnetic (FM) and metallic state in the vicinity of the FM transition of manganites, is generally explained by the double-exchange model.[1,2] However, many findings in the transport, magnetic, and structural properties have revealed that orbital degree of freedom, Coulomb repulsive interaction, Jahn–Teller effect, and superexchange interaction also play very important roles in the CMR effect.[3,4] In doped manganites, the FM metallic state is realized by the coupling of mobile e_g orbital carriers with local t_{2_g} orbital spins. As the transfer interaction or the one-electron bandwidth (W) of the e_g carriers decreases, which depends on the Mn–O–Mn bond angle in the perovskites, the FM state will suffer from the competing instabilities such as charge ordering, orbital ordering, or collective Jahn–Teller distortions.[3,5] The one-electron bandwidth can be changed by the mean radius of *A* site cations, resulting in lattice distortions. There are two types of the charge ordering (CO) transition. One (type I) is the CO state emerging in the FM phase, where the CO instability is not strong,[6] and the other (type II) is the CO state occuring at a higher temperature, where the FM phase is no longer present.[7] $Nd_{1-x}Sr_xMnO_3$ shows complex phase transitions and belongs to the type I CO state at $x=0.5$.[6] For $0.3<x<0.48$, the compounds show a FM metallic state as the ground state, and in the region of $0.50\leqslant x\leqslant 0.60$, they are in a metallic antiferromagnetic (AF) phase with a layered *A*-type spin structure.[8,9] With further increase of x, they are in another AF phase with a *C*-type spin structure.[9] In a very narrow composition range of around $x\sim 0.5$, on cooling from room temperature, the compound shows a transition from a paramagnetic state to a FM state at about 250 K and then a transition from FM state to a CO insulator with charge exchange (CE)-type AF spin structure below 160 K.[8–10] The crystal structures of the CE-type and *A*-type AF states are characterized by apically compressed MnO_6 octahedra, while that of the *C*-type AF state is characterized by apically elongated octahedra, reflecting their respective layered-type or rod-type orbital ordering patterns.[9] Moritomo *et al.*[11] determined the space group of $Nd_{0.5}Sr_{0.5}MnO_3$ to be *Pbmn*, which is much more common in perovskites, and this symmetry has been assumed in several subsequent articles.[8,12–14] On the other hand, recently, Woodward *et al.*[10] reported that two samples with the same composition of $Nd_{1/2}Sr_{1/2}MnO_3$ prepared in a similar manner but using different starting materials show different phase transitions during cooling of the samples. According to the analyses of high-resolution synchrotron x-ray diffraction and neutron diffraction, they found that one of the samples undergoes a phase transition from an

a)Electronic mail: rcyu@aphy.iphy.ac.cn

orthorhombic phase (FM) with *Imma* symmetry to another orthorhombic one (*A*-type AF) with the same symmetry at about 225 K, and then a transition from the *A*-type AF orthorhombic to a monoclinic CO phase (CE-type AF) with $P2_1/m$ symmetry at about 150 K. But these three phases can coexist even at a temperature as low as 15 K. However, the other sample only shows a transition from orthorhombic FM to CE-type AF monoclinic phase at about 150 K without observation of the *A*-type AF phase. They explained the different behaviors between the two samples by the slight excess of Mn^{4+} and a wider compositional range for the first sample than for the second one. There are three ground states around $x=0.5$, indicating that the three phases have approximately same energies. Thus, small energy disturbance, for example, caused by temperature, magnetic field,[15,16] strain,[17,18] and high pressure,[19–21] etc., can give rise to phase transitions among them.

High pressure, as one of thermodynamic parameters, influences the charge, spin, and/or orbital ordering of a sample. Moritomo *et al.*[19] reported that hydrostatic pressure (<1 GPa) increases T_C and decreases T_{CO} in single crystal $Nd_{0.5}Sr_{0.5}MnO_3$, while Arima and Nakamara[20] reported that uniaxial pressure along the *c* axis decreases T_C and increases T_{CO} in the same crystal, and stabilizes the *A*-type AF state with increasing T_N in single crystal $Nd_{0.45}Sr_{0.55}MnO_3$. Recently, Cui et al.[21] have investigated the transport and structural properties of pressure-induced magnetic states in polycrystalline $Nd_{0.5}Sr_{0.5}MnO_3$ and found that the T_{CO} increases first with increasing pressure and appears to decrease at pressures above ~3.8 GPa.

In this article, we report the transport and magnetic properties of the polycrystalline bulk $Nd_{0.5}Sr_{0.5}MnO_3$ at ambient pressure and the transport property under hydrostatic pressures up to 7.5 GPa generated by a large cubic anvil apparatus. Possible orbital ordering behavior in the sample under high pressure has been conjectured.

II. EXPERIMENTS

The polycrystalline bulk $Nd_{0.5}Sr_{0.5}MnO_3$ was prepared using a traditional solid state reaction technique. Stoichiometric amounts of Nd_2O_3, $SrCO_3$, MnO_2, and Mn_2O_3 powders were mixed, ground, pelletized, and calcined three times at 1050 °C in air for 24 h with intermediate grindings. The pellets thus obtained were reground, pelletized, and sintered at 1350 °C in air for 48 h, and then cooled to room temperature in a furnace. Transport and magnetic properties of the samples were measured using a Mag Lab System (Oxford, U.K., 2000), and the electrical resistivity of $Nd_{1-x}Sr_xMnO_3$ ($x\sim0.5$) under high pressures was measured as a function of temperature by means of the dc four-probe method using the cubic anvil apparatus operated up to 7.5 GPa. The cubic anvil high pressure device was compressed evenly from six directions with six anvil tops, thereby producing a hydrostatic high pressure for a sample sealed in the gasket. Two of the six anvil tops were fixed to metal molds placed at upper and lower sections. The anvil top was made of tungsten carbide, and the gasket material was a mixture of amorphous boron and epoxy resin in 4:1 weight ratio. In the gasket there was a Teflon inner cell used to contain the sample tested. Fluorinert liquid was used as the pressure medium. Low temperatures down to 78 K were attained by a continuous flow of liquid nitrogen.

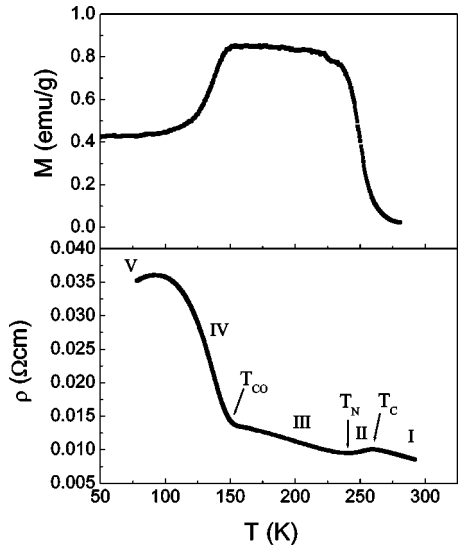

FIG. 1. (a) Temperature dependence of: magnetization (upper panel) and resistivity (lower panel) of $Nd_{0.5}Sr_{0.5}MnO_3$ at ambient pressure. The notations I, II, III, and IV represent the PM, FM, *A*-type AF, and CO CE-type AF regions, respectively. The decrease of resistivity in region V indicates the coexistence of the FM and CO CE-type AF phases at low temperatures. T_N and T_{CO} denote the *A*-type AF and CO CE-type AF transition temperatures, respectively.

III. RESULTS AND DISCUSSION

The phase structure of the prepared polycrystalline sample $Nd_{0.5}Sr_{0.5}MnO_3$ was checked by x-ray powder diffraction and determined to be an orthorhombic structure with *Imma* symmetry. The refined unit cell parameters are $a=0.5432$ nm, $b=0.5470$ nm, and $c=0.7685$ nm, in agreement with the results reported in Ref. 10. No impurity was detected within the measuring accuracy of the detector.

Temperature dependences of magnetization and resistivity are shown in Figs. 1(a) and 1(b), respectively. Both measurements were performed in the warming course. The $R-T$ curve plotted in Fig. 1(b) can be divided into five regions, as marked in the figure. It shows a transition from a paramagnetic (PM) state in region I to a FM state in region I at T_C about 258 K. In region I, the resistance decreases with increasing temperature, showing a semiconducting behavior, while in region II, on the contrary, the resistance increases with increasing temperature, showing a metallic behavior. This transition is in agreement with that reported by other researchers[6,8,22] though the T_C in this article is a little higher. With decreasing temperature, there is a FM to *A*-type AF transition at about 236 K (T_N), going from region II to region III. A similar transition was also observed in $Nd_{0.45}Sr_{0.55}MnO_3$ at around 225 K,[8,10,23] in $Nd_{0.49}Sr_{0.51}MnO_3$ at about 200 K,[9] and in $Nd_{0.49}Sr_{0.51}MnO_3$ below 200 K.[14] With further decreasing temperature, a CO CE-type AF state occurs below about 150 K and the resistivity increases more steeply in region IV with decreasing temperature. In region V where the temperature is below about 91 K, the resistivity

decreases with decreasing temperature, showing metallic behavior. As determined by neutron diffraction experiements,[24,8–10] the *A*-type AF has a layered spin structure with $d(x^2-y^2)$ orbital ordering, where the spins couple with each other ferromagnetically in the *ab* plane and antiferromagnetically along the *c* axis. It is also predicted theoretically that this spin ordering should be accompanied by the $d(x^2-y^2)$ type FM orbital ordering.[25,26] However, the CE-type AF state has an AF spin structure with $d(3x^2-r^2)/d(3y^2-r^2)$ orbital ordering accompanying the CO state. The behavior of our sample is markedly different from that reported for single crystal $Nd_{0.5}Sr_{0.5}MnO_3$ by Kuwuhara *et al.*[6] and Kawano *et al.*[8] in which a sharp transition from the FM to the CE-type AF phase was observed at ~160 K without observation of the *A*-type AF phase, but our result is consistent with the phase segregation results reported in Refs. 10 and 16. Ritter *et al.*[16] reported that at $H=0$ and 125 K, $Nd_{0.5}Sr_{0.5}MnO_3$ would segregate into two different crystallographic structures with three magnetic phases: i.e., orthorhombic (*Imma*) FM (19%), orthorhombic (*Imma*) *A*-type AF (21.6%), and monoclinic ($P2_1/m$) CO CE-type AF (59.4%) phases. Woodward *et al.*[10] reported that very small changes in the $Mn^{4+}:Mn^{3+}$ ratio caused by either cation vacancies or oxygen off stoichiometry could stabilize the FM state when $Mn^{4+}:Mn^{3+}<1$, and stabilize the *A*-type AF state when $Mn^{4+}:Mn^{3+}>1$ in the CO phase, which would give rise to phase segregation. Due to the ferromagnetic coupling of spin and orbital in the *ab* plane in the *A*-type AF structure, the transport property is anisotropic. Kuwahara *et al.*[27] reported on the metallic transport property in the *ab* plane and insulating behavior along the *c* axis in the *A*-type AF $Nd_{0.45}Sr_{0.55}Mn_{O_3}$ crystal. The metallic behavior is also reported in Ref. 23. But in our experiments, the transport property shows semiconducting behavior in the *A*-type AF phase, which might be due to the polycrystalline bulk sample used in our case. Such behavior was also observed by Moritomo *et al.*[14] in $Nd_{0.48}Sr_{0.52}MnO_3$ and Kajimoto *et al.*[9] in $Nd_{0.49}Sr_{0.51}MnO_3$. But it can be seen from Fig. 1 that the change of the resistivity versus temperature is slower in the *A*-type AF state than that in the CE-type state. Due to the emergence of the FM order that coexists with the CE-type AF spin order, the increase of the resistivity is suppressed below ~91 K in region V. Such a behavior was also observed by Kajimoto *et al.*[9] in $Nd_{0.51}Sr_{0.49}Mn_{O_3}$. The phase segregation in our sample may be caused by either the slightly inhomogeneous composition in the sample or the intrinsic nature due to approximately the same free energies of the three phases. Correspondingly, the temperature dependence of the magnetization ($M-T$) curve presented in Fig. 1(a) shows different features with the variation of temperature. With decreasing temperature, the magnetization (M) increases at T_C (258 K) due to the transition from PM to FM state, and appears a little fluctuant at T_N (236 K). At T_{CO} (153 K), the M value starts to decrease and then keeps almost the same value below 91 K, thus verifying the coexistence of the FM and CO phases at low temperatures. The behavior of the measured $M-T$ curve can be well explained with the viewpoint of phase segregation.

Figure 2 shows the resistance versus temperature under hydrostatic pressures up to 7.5 GPa. Only the CO transition is seen in the data obtained at 1.5 GPa without the appearance of the FM state. The CO transition temperature at 1.5 GPa is a little higher than that at ambient pressure. With increasing pressure up to 3.0 GPa, the CO transition temperature also increases while the resistance decreases in the whole temperature range, showing an increased transport property under high pressure. With further increasing pressure to and above 4.5 GPa, it is impossible to determine the T_{CO}, which distinguishes the *A*-type and CE-type AF regions, and the resistance is further reduced in the whole temperature range. The temperature dependence of the resistance displays an *A*-type AF character at and above 4.5 GPa. According to the results shown in Fig. 2, we conjecture and propose a possible scenario of phase transition under high pressure for the sample studied, as shown in Fig. 3. As mentioned above, there exist very close correlations among the FM, *A*-type AF, and CE-type AF states. With increasing pressure, at the beginning stage both the CO CE-type AF and *A*-type AF states are favored simultaneously at lower pressures, while the FM phase is suppressed. But later at higher pressures, the *A*-type AF phase grows at the expense of the CE-type ordered region. In our experiments, the FM phase is suppressed at below 1.5 GPa, accompanied by the vanishing of the metallic transport behavior in the temperature range of 236–258 K as well as below 91 K. In the normal case, high

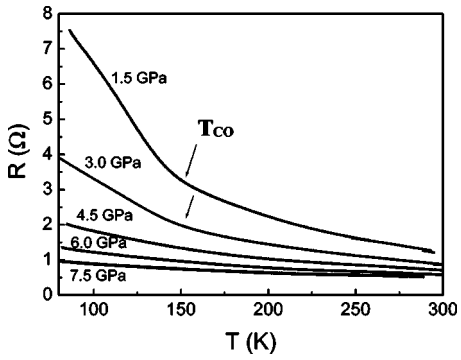

FIG. 2. Resistance vs pressure curves at different hydrostatic pressures up to 7.5 GPa. The CO CE-type transition temperature T_{CO} is marked with arrows.

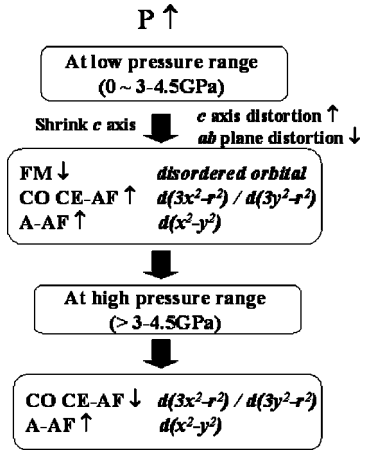

FIG. 3. Schematic view of the changes of different magnetic structures in $Nd_{0.5}Sr_{0.5}MnO_3$ under high pressures.

pressure increases the one-electron bandwidth and enhances the itineracy of e_g electrons through changing the Mn–O–Mn bond angle and Mn–O bond length, and suppresses the CO state and favors the FM phase.[19] The suppression of CO states under high pressure was also observed in many other perovskites. For example, Moritomo *et al.*[11] reported that high pressure suppresses the CO state of the $Pr_{1-x}Ca_xMnO_3$ compounds ($x=0.35, 0.4, 0.5$), which have a narrow one-electron bandwidth, and it also induces a metallic transition from a CO insulator to a FM metallic phase. In contrast to the normal case, there are also some examples in which high pressure increases T_{CO} and decreases T_C, thus the CO state is favored while the FM state is suppressed. For example, Arima and Nakamura *et al.*[20] reported that the uniaxial pressure along the *c* axis raises the charge and orbital ordering temperature in the $Nd_{0.5}Sr_{0.5}MnO_3$ compound. Moritomo *et al.*[11] reported that with increasing pressure, the resistivity is suppressed and T_{CO} gradually increases in the compound $(Nd_{0.6}La_{0.4})Sr_{0.5}MnO_3$ with increased bandwidth and they suggested a transition from the CO CE-type AF to the *A*-type AF state. The phenomenon of pressure-enhanced T_{CO} transition was also observed in $(Nd_{0.5}Sm_{0.5})Sr_{0.5}MnO_3$.[19] Recently, Cui *et al.*[21] found that in polycrystalline $Nd_{0.5}Sr_{0.5}MnO_3$ the T_{CO} would increase with pressure below 3.8 GPa but decrease above this pressure. Consistent with the results in Ref. 21, the T_{CO} also increases with pressure below 3–4.5 GPa in our experiment, but we have not observed the decrease of T_{CO} at higher pressures due to the suppression of the CE-type AF state. There are some differences between the two experiments. For example, their sample only shows FM and CO CE-type transitions with decreasing temperature, while ours show FM, *A*-type AF and CE-type AF transitions. Besides, the T_{CO} is defined as the transition point of the FM and CE-type AF states in their resistivity curve, while it is defined as the transition point of the CE-type AF and *A*-type AF phases in our case. Similar to the uniaxial case, in our experiment the hydrostatic pressure may increase the *c*-axis distortion and decrease the distortion in the *ab* plane. Since the CO state corresponds to a higher orthorhombic distortion state[6] and has a CE-type AF spin structure with $d(3x^2-r^2)/d(3y^2-r^2)$ orbital ordering, it is favored under high pressures due to the shrinkage of the *c* axis, whereas the FM state with disordered orbital ordering is suppressed. The shrinkage of the *c* axis also favors the *A*-type AF state due to its $d(x^2-y^2)$ orbital ordering. The increase of the *c*-axis distortion and decrease of the distortion in the *ab* plane in $Nd_{0.5}Sr_{0.5}MnO_3$ with variation of pressure have also been observed by Cui *et al.*[21] through structural measurements. Kawano *et al.*[8] reported that the *c* parameter of the orthorhombic cell shrinks about 1% at the CO transition temperature accompanied by the cooperative Jahn–Teller distortion in $Nd_{0.5}Sr_{0.5}MnO_3$ and 2.7% at the *A*-type AF transition $T_N \sim 230$ K in $Nd_{0.45}Sr_{0.55}MnO_3$. Woodward *et al.*[10] analyzed the cell volumes at 100 K and below, and found that the cell volume is systematically larger than the weighted average volume, which is essentially the same as that of CE-type AF phase, while the cell volume of the *A*-type AF phase is significantly smaller than the average volume. So it is reasonable that high pressure prefers the CE-type AF and *A*-type AF states to the FM state at the initial stage, and finally favors the *A*-type AF and suppresses the CE-type AF state. Also high pressure can widen the one-electron bandwidth, and this is also a possible factor to favor the *A*-type AF phase with $d(x^2-y^2)$ orbital ordering under high pressure at the final stage.[8] In both the CE-type and *A*-type states, resistivity is reduced due to the enhanced *ab*-plane transfer integral by the reduction of *ab*-plane distortion,[21] so the decrease of resistance under high pressure is always observed in the whole measuring range of temperature.

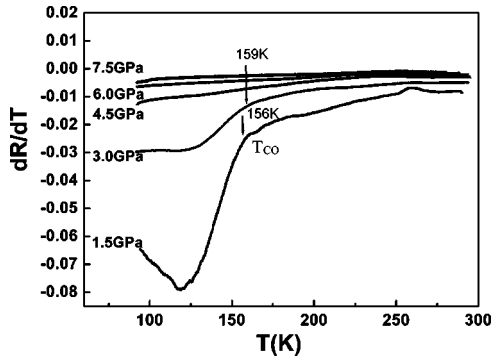

FIG. 4. The curves of first-order derivative of resistance vs temperature. The CO CE-type transition temperature T_{CO} is marked with arrows.

In order to see clearly the change of T_{CO}, we present the derivative of resistance versus temperature in Fig. 4 and mark the T_{CO} with arrows. The increase of T_{CO} is obviously seen. As described above, the curve for 4.5 GPa changes placidly, implying the suppression of the CO CE-type AF state and the domination of the *A*-type AF phase at this pressure. The curves corresponding to 6.0 and 7.5 GPa are more complanate, indicating an enhanced charge transfer under higher pressures.

As mentioned above, there are several magnetic structures with different orbital ordering. Such phase segregation looks more complicated, but it is more meaningful to study the effect of high pressure, for example, more clear sequence of the change of the different magnetic structures when they coexist.

Generally magnetic field reduces the resistance of many doped perovskite manganites due to the enhanced double exchange interaction, and magnetoresistance (MR) can be defined as $MR=(\rho(T,0)-\rho(T,H))/\rho(T,0)$, where H denotes the external field and $\rho(T,0)$ and $\rho(T,H)$ represent the resistivities at zero and H fields, respectively. Due to the change of charge, spin, and orbital ordering under high pressures, the transport property will also be changed with pressure. In a similar way, we also can define the pressure-induced resistance change (PR) as $PR=(\rho(T,0)-\rho(T,P))/\rho(T,0)$, where P denotes the external pressure and $\rho(T,0)$ and $\rho(T,P)$ represent the resistivities at ambient and P pressures, respectively. Since the measurements at ambient pressure and high pressures in our experiment are carried out using two pieces of the same sample, we replace $\rho(T,0)$ with $\rho(T,1.5\ \text{GPa})$ to calculate PR in this article. The curves of calculated PR value versus temperature at different pressures are shown in Fig. 5. Large PR values are observed in the whole temperature range and the PR increases with pressure at a constant

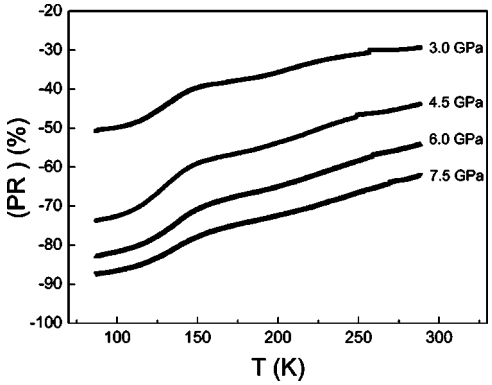

FIG. 5. Temperature dependence of calculated PR values at different pressures

temperature. It can be imagined that the PR value will be increased much more if it is calculated by using $\rho(T,0)$.

IV. CONCLUSIONS

The $Nd_{0.5}Sr_{0.5}MnO_3$ synthesized by solid-state reaction shows FM, *A*-type AF, and CE-type AF transitions with decreasing temperature. Such complex phase transitions are considered to be caused by phase segregation owing to the possible cation vacancies and/or oxygen content off stoichiometry. It is conjectured that at the beginning stage, at lower pressure, high pressure favors the *A*-type AF phase with $d(x^2-y^2)$ orbital ordering and the CO CE-type AF phase with $d(3x^2-r^2)/d(3y^2-r^2)$ orbital ordering, while it suppresses the FM phase with disordered orbital ordering. At the much later stage at higher pressures, the *A*-type AF phase is the dominant one with the suppression of CE-type AF phase. The decrease of resistance in the whole temperature range under high pressures is due to the enhanced itineracy of e_g electrons in the *ab* plane, caused by the increased transfer integral under high pressures. PR is defined in a way similar to MR, and shows large negative values under high pressures.

ACKNOWLEDGMENTS

This work was supported by the National Natural Science Foundation of China (Grant Nos. 10274099, 50321101, and 50332020), the State Key Development Program for Basic Research of China (Grant No. 2002CB613301) and the Japan Society for the Promotion of Science Project. R. C. Yu acknowledges the support from the Berkeley Scholar Program.

[1]C. Zener, Phys. Rev. **82**, 403 (1951).
[2]P. W. Anderson and H. Hasegawa, Phys. Rev. **100**, 675 (1955).
[3]A. J. Millis, P. B. Littlewood, and B. J. Shrainman, Phys. Rev. Lett. **74**, 5144 (1995).
[4]S. Ishihara, J. Inoue, and S. Maekawa, Phys. Rev. B **55**, 8280 (1997).
[5]H. Röder, J. Zang, and A. R. Bishop, Phys. Rev. Lett. **76**, 1356 (1996).
[6]H. Kuwahara, Y. Tomioka, A. Asamitsu, Y. Moritomo, and Y. Tokura, Science **270**, 961 (1995).
[7]Y. Tomioka, A. Asamitsu, H. Kuwahara, Y. Moritomo, and Y. Tokura, Phys. Rev. B **53**, R1689 (1996).
[8]H. Kawano, R. Kajimoto, H. Yoshizawa, Y. Tomioka, H. Kuwahara, and Y. Tokura, Phys. Rev. Lett. **78**, 4253 (1997).
[9]R. Kajimoto, H. Yoshizawa, H. Kawano, H. Kuwahara, Y. Tokura, K. Ohoyama, and M. Ohashi, Phys. Rev. B **60**, 9506 (1999).
[10]P. M. Woodward, D. E. Cox, T. Vogt, C. N. R. Rao, and A. K. Cheetham, Chem. Mater. **11**, 3528 (1999).
[11]Y. Moritomo, H. Kuwahara, Y. Tomika, and Y. Tokura, Phys. Rev. B **55**, 7549 (1997).
[12]H. Kuwahara, Y. Moritomo, Y. Tomioka, A. Asamitsu, M. Kasai, R. Kumai, and Y. Tokura, Phys. Rev. B **56**, 9386 (1997).
[13]T. Akimoto, Y. Maruyama, Y. Moritomo, A. Nakamura, K. Hirota, K. Ohoyama, and M. Ohashi, Phys. Rev. B **57**, R5594 (1998).
[14]Y. Moritomo, T. Akimoto, A. Nakamura, K. Ohoyama, and M. Ohashi, Phys. Rev. B **58**, 5544 (1998).
[15]R. Mahendiran, M. R. Ibarra, A. Maignan, F. Millange, A. Arulraj, R. Mahesh, B. Raveau, and C. N. R. Rao, Phys. Rev. Lett. **82**, 2191 (1999).
[16]C. Ritter, R. Mahendiran, M. R. Ibarra, L. Morellon, A. Maignan, B. Raveau, and C. N. R. Rao, Phys. Rev. B **61**, R9229 (2000).
[17]W. Prellier, A. Biswas, M. Rajeswari, T. Venkatesan, and R. L. Greene, Appl. Phys. Lett. **75**, 397 (1999).
[18]Q. Qian, T. A. Tyson, C.-C. Kao, W. Prellier, J. Bai, A. Biswas, and R. L. Greene, Phys. Rev. B **63**, 224424 (2001).
[19]Y. Moritomo, H. Kuwahara, and Y. Tokura, J. Phys. Soc. Jpn. **66**, 556 (1997).
[20]T. Arima and K. Nakamura, Phys. Rev. B **60**, R15013 (1999).
[21]C. W. Cui, T. A. Tyson, Z. Q. Chen, and Z. Zhong, Phys. Rev. B **68**, 214417 (2003).
[22]K. Nakamura, T. Arima, A. Nakazawa, Y. Wakabayashi, and Y. Murakami, Phys. Rev. B **60**, 2425 (1999).
[23]H. Yoshizawa, H. Kawano, J. A. Fernandez-Baca, H. Kuwahara, and Y. Tokura, Phys. Rev. B **58**, R571 (1998).
[24]E. O. Wollan and W. C. Koehler, Phys. Rev. **100**, 545 (1955).
[25]R. Maezono, S. Ishihara, and N. Nagaosa, Phys. Rev. B **58**, 11583 (1998).
[26]S. Okamoto, S. Ishihara, and S. Maekawa, Phys. Rev. B **61**, 14647 (2000).
[27]H. Kuwahara, T. Okuda, Y. Tomioka, A. Asamitsu, and Y. Tokura, Phys. Rev. Lett. **82**, 4316 (1999).